Joint Optimization of Trajectory Planning and Task Scheduling in Heterogeneous Multi-UAV System

Add your name and affiliation as Author

Abstract

The use of unmanned aerial vehicles (UAV) as a new sensing paradigm is emerging for surveillance and tracking applications, especially in the infrastructure-less environment. One such application of UAVs is in the construction industry where currently prevalent manual progress tracking results in schedule delays and cost overruns. In this paper, we develop a heterogeneous multi-UAV framework for progress tracking of large construction sites. The proposed framework consists of $Edge\_UAV$ which coordinates the data relay of the visual sensor-equipped Inspection UAVs (I_UAVs) to the cloud. Our framework jointly takes into consideration the trajectory optimization of the $Edge\_UAV$ and the stability of system queues. In particular, we develop a Distance and Access Latency Aware Trajectory (DLAT) optimization that generates a fair access schedule for I_UAVs. In addition, a Lyapunov based online optimization ensures the system stability of the average queue backlogs for data offloading tasks. Through a message based mechanism, the coordination between the set of I_UAVs and $Edge\_UAV$ is ensured without any dependence on any central entity or message broadcasts. The performance of our proposed framework with joint optimization algorithm is validated by extensive simulation results in different parameter settings.

Keyword: Path Planning, Task Scheduling, Data Offloading, Construction Site Monitoring, Unmanned Aerial Vehicles (UAVs), Lyapunov Optimization

1 Introduction

The unmanned aerial vehicle (UAV) based solutions are emerging in various domains such as wireless sensing [1], payload delivery [2], precision agriculture [3], help and rescue operations [4], etc. Moreover, with the current trend of automation, sensing and information exchange in Industry 4.0, UAV based applications are also finding their place in the construction industry especially for resource tracking and progress monitoring using aerial imagery. Such solutions are helpful in infrastructure-less large construction sites as they provide ease of deployment, quick access to the ground-truth data and higher reachability and coverage [5]. Further, the autonomous or semi-autonomous UAV based solutions could facilitate progress monitoring, building inspections (for cracks or other defects), safety inspections (to find any environmental hazards) and many more construction-specific audits automatically. The UAV based visual monitoring of under-construction projects also allows simultaneous observability of ground-truth data by different collaborating entities. Availability of such data and information helps in timely assessments that could reduce schedule delays, cost overruns, resource wastage and financial losses which are not uncommon in construction projects.

A plausible solution to address the aforementioned challenges could be a Mobile Edge Computing (MEC) [6] based heterogeneous multi-UAV framework. Such a framework along with the prior geometric knowledge available about the construction site as gathered from a Building Information Model (BIM)[7] could help create an effective multi-UAV based visual monitoring system for construction sites. As for any constrained environment, the optimization of computational resources is central to develop a solution. The integration of UAVs and MEC into a single framework could facilitate that with efficient data collection/processing from the UAV based dynamic sensors in infrastructure-less environments [8]. In addition, an MEC based framework can help to perform partial computation offloading wherein a part of data is processed by the UAVs while the rest gets offloaded to the cloud.

An MEC based UAV framework is not new and the deployment of the UAVs as base stations or edge servers is widely studied [9, 10]. These studies reflect on the

flexibility in deployment of UAV based edge computing components. However, there is a problem of buffer overflow of UAVs due to the limited on-board processing and the shared bandwidth to transfer data to the cloud which leads to instability in the system. In addition, the dynamic nature of such systems with varying data traffic and continuous movement of UAVs makes it difficult to stabilize or control the system in a deterministic manner. Researchers have used online Lyapunov optimization [11] to address such system instabilities. Lyapunov optimization considers the stability of the system with time varying data and optimizes time averages of system utility and queue backlogs.

In this paper, we address the challenges of deploying a heterogeneous multi-UAV system for construction site monitoring by the joint optimization of UAV trajectory planning and data offloading task scheduling. The proposed framework employs two types of UAVs viz. Inspection UAVs I_UAVs and Mobile Edge UAVs ($Edge\_UAV$). While the former is deployed as visual sensors to collect visual data from different locations of the site, the latter interacts and collects data from I_UAVs, and offloads the same to the cloud. The core objective of the framework is to minimize the total energy consumption of the system while considering the data queue backlogs of I_UAVs and $Edge\_UAV$ and also jointly optimizing the trajectory of the $Edge\_UAV$ in accordance with the trajectories of I_UAVs having minimum access latency and travel distance. The online resource management such as transmission power and processor frequency of the $Edge\_UAV$ is evolved using Lyapunov optimization (as in [12]).

The rest of the paper is organised as follows: Section 2 presents the proposed heterogeneous multi-UAV framework for construction site monitoring. The overall system objective is discussed in Sections 3. Sections 4 and 5 discuss the trajectory optimization and Lyapunov based system stability, respectively. The simulation setup has been presented in Section 6. Section 7 discusses the results gathered from the experiments while Section 8 concludes the paper.

2 Heterogeneous Multi-UAV Framework

Figure **??** depicts the overall multi-UAV framework with all its components. The system consists of two heterogeneous UAVs i.e. a set of Inspection UAVs $I\_UAV = \{I\_UAV_1, I\_UAV_2, I\_UAV_3, ..., I\_UAV_N\}$ and a Mobile Edge UAV ($Edge\_UAV$). I_UAVs are smaller in size and are more agile. They collect visual data from a set of Point of Interests (PoIs) denoted as $L = \{l_1, l_2, l_3....l_k\}$ across the construction site. As the construction sites are infrastructure-less environments, there are limited Access Points (AP) available for connectivity to the cloud. Further, the I_UAVs possess limited connectivity range that makes it difficult for them to transfer data to cloud directly. In addition, the I_UAVs move in the 3D Cartesian coordinate system. The $Edge\_UAV$, which is larger in size and possesses higher computational capabilities, coordinates with the I_UAVs to relay the data (after partially processing the same) to the cloud. $Edge\_UAV$ always maintains a constant height and thus its trajectory lies in an horizontal plane.

The communication between I_UAV and $Edge\_UAV$ (A2A channel) has limited range and bandwidth. We have assumed the achievable data transmission rate of the I_UAV_i in a given time slot as $d_i^{off}(t)$. Further, The height of the $Edge\_UAV$ is h which is dependent on coverage range r and line of sight (LoS) loss caused due to environmental effects [13].

The A2A channel power gain (ζ) from I_UAV to $Edge\_UAV$ can be given as:

$$\zeta = g_0 * (\frac{dis_0}{dis_t})^\theta \tag{1}$$

where g_0 is the path loss constant, dis_0 is the reference distance, dis_t distance between the UAVs, and θ is the path loss exponent.

2.1 Data collection and offloading

Each PoI (l_i) is a tuple ($< d_i, \psi_i >$) where d_i specifies the amount of data (images) to be collected and ψ_i denotes the coordinates of the site locations in 3D space. The sequence of PoIs to be visited is provided to I_UAVs and same is also shared with the $Edge\_UAV$. During the traversal along the sequence of PoIs, the limited buffer may make the I_UAV wait at some PoIs along the trajectory until it offloads the data to the $Edge\_UAV$.

The $Edge\_UAV$ can communicate with one of the I_UAV_i in a time slot. The data gathered by each of the I_UAV_i in a time slot t is denoted by $A_i(t)$. $Q_i(t)$ represents the queue of the I_UAV_i and $d_i^{off}(t)$ denotes

the amount of data offloaded to the $Edge\_UAV$ by the I_UAV_i in time-slot t. The recursive equation to update the $Q_i(t)$ is as follows:.

$$Q_i(t+1) = max\{Q_i(t) - d_i^{off}(t), 0\} + A_i(t) \quad (2)$$

The $Edge\_UAV$ accepts data from the selected I_UAV_i in the time-slot t in its queue $L(t)$. The following equation updates $L(t)$ recursively:

$$L(t+1) = max\{L(t) - c(t) - d_{edge}^{off}(t), 0\} + A_{edge}(t) \quad (3)$$

where $A_{edge}(t)$ is the data arrived from the selected I_UAV_i in time-slot t, $c(t)$ is the data processed by the $Edge\_UAV$ in time-slot t, and $d_{edge}^{off}(t)$ is the number of bits offloaded to the cloud in time-slot t.

3 System Objective

In the proposed framework, the offloading of data happens at two stages - 1) from I_UAV_i to $Edge\_UAV$ and 2) from $Edge\_UAV$ to the cloud. Our main focus is to achieve the end-to-end data offloading to the cloud by minimizing the total energy consumption of the whole system (E_{system}) which is defined as:

$$E_{system}(t) = E_{edge}^{transition}(t) + E_{edge}^{Comm}(t) + \left(\sum_{i=1}^{N}(E_i^{Comm}(t))\right) \quad (4)$$

where $E_{edge}^{transition}(t)$ is the transition energy of the $Edge\_UAV$, $E_{edge}^{Comm}(t)$ is a communication energy of the $Edge\_UAV$ and $E_i^{Comm}(t)$ is the communication energy of the $i^{th} I\_UAV_i$.

Further, we discuss the various components of E_{system} along with the expressions to calculate the same.

3.0.1 Transition energy of $Edge\_UAV$

The transition energy of $Edge\_UAV$ refers to the energy consumed in moving from one location to another. The transition energy of the $Edge\_UAV$ is given as:

$$E_{edge}^{transition} = \kappa ||vel(t)||^2 \quad (5)$$

where κ is a constant that depends on the total mass of the $Edge\_UAV$ and $vel(t)$ is the velocity of I_UAV

3.0.2 Communication energy of $Edge\_UAV$

$Edge\_UAV$ offloads the data to cloud through a wireless channel [14]. The communication energy consumed to transmit the data to the cloud is given as:

$$E_{edge}^{comm}(t) = (2^{\frac{d_{edge}^{off}(t)}{W*\tau}} - 1) * \frac{N_0 W}{\zeta} * \tau \quad (6)$$

where the parameters are defined in the Table **??**

3.0.3 Communication Energy of I_UAV

The energy consumed for offloading the $d_i^{off}(t)$ data bits at time slot t from the selected I_UAV_i to the $Edge\_UAV$ using the A2A channel of bandwidth W Hz is given similarly to Equation 6 as:

$$E_i^{comm}(t) = (2^{\frac{d_i^{off}(t)}{W*\tau}} - 1) * \frac{N_0 W}{\zeta} * \tau \quad (7)$$

As the PoIs are predefined and the I_UAVs follow a predetermined path, the energy consumed for the movement of I_UAVs are not taken into consideration.

Given the energy of the system, our goal is to find the optimal parameter values so as to minimize the expected cumulative energy across the time horizon. The system policy in every time-slot t can be given by $X(t) = \{F_{edge}(t), p_i(t), P_{edge}(t), S_{edge}(t)\}$. Hence, the end-to-end data offloading policy parameters $X(t)$ aims at minimizing total expected energy of the system. As the channel information for the data offloading is not deterministic and varies in the environment, the amount of bits arrived at the $Edge\_UAV$ depends upon the channel characteristics as well as the current position of the selected I_UAV_i. Such time-coupling of variables is responsible for the stochastic nature of the system. The overall optimization model for the stable system performance is given as:

$$\textbf{P1:} \quad \min_{X(t)} \lim_{T\to\infty} \frac{1}{T}\sum_{t=1}^{T} \mathbb{E}[E_{system}(t)]$$

s.t.

$$0 \le F_{ME}(t) \le Fmax \quad t\epsilon T \quad (C1)$$
$$0 \le p_i(t) \le p_{i,max} \quad i = 1...N \quad t\epsilon T \quad (C2)$$
$$0 \le P_{edge}(t) \le P_{max} \quad t\epsilon T \quad (C3)$$
$$d_i^{off}(t) \le Q_i(t) \quad i = 1..N \quad t\epsilon T \quad (C4)$$
$$c(t) \le \frac{F_{max}\tau}{\rho_{edge}} \quad t\epsilon T \quad (C5)$$
$$d_i^{off} \le W\tau log_2(1 + \frac{(\zeta)p_{i,max}(t)}{N_o * W}) \quad i = 1..N \quad t\epsilon T \quad (C6)$$
$$d_{edge}^{off}(t) \le W\tau log_2(1 + \frac{\zeta P_{max}(t)}{N_o W}) \quad t\epsilon T \quad (C7)$$
$$\lim_{T\to\infty} \frac{\mathbb{E}[Q_i(t)]}{T} = 0 \quad i = 1..N \quad t\epsilon T \quad (C8)$$
$$\lim_{T\to\infty} \frac{\mathbb{E}[L(t)]}{T} = 0 \quad t\epsilon T \quad (C9)$$

The constraints $C1$ and $C3$ defines the maximum frequency and maximum transmission power of the $Edge\_UAV$ respectively. In addition, $C5$ defines the maximum number of bits processed by $Edge\_UAV$. Furthermore, $C4$ and $C6$ upper bound the number of transmitted bits. Similarly, for I_UAV, the constraints $C2$, $C4$ and $C6$ bound the number of transmitted bits. The constraints $C8$ and $C9$ establish the rate stability of all system queues (I_UAV_i and $Edge\_UAV$). Next we discuss the model to optimize the trajectory of the $Edge\_UAV$ with respect to the trajectories of I_UAVs.

4 Distance and Latency Aware Trajectory

The flexible and dynamic trajectory planning of $Edge\_UAV$ could help in applications within construction industry where it is hard to reach by terrestrial communication infrastructure. As already mentioned, the position of I_UAVs changes in every time-slot since they move through different PoIs to collect data. Hence, the $Edge\_UAV$'s trajectory needs to be estimated in such a manner that it can connect and access an I_UAV_i in a time-slot before the I_UAV_i's queue overflows. Whenever an I_UAV_i's queue gets full, it doesn't move to its next designated PoI and sojourns at the same PoI until it is able to offload its data to the $Edge\_UAV$ and free up some queue space. Hence, in order to choose one of the I_UAVs to offload its queue, the $Edge\_UAV$ would require the real-time information about the queues of all the I_UAVs in each time-slot. This information is not available a priori due to the dynamic nature of the system. We use a message passing based approach for estimating the queue sizes of the I_UAVs in order to make a selection. Further, the trajectory of the $Edge\_UAV$ must be optimized so as to consume minimal energy. The trajectory optimization model of $Edge\_UAV$ optimizes the trade-off between transition energy of $Edge\_UAV$ and access latencies of all I_UAV_is. In addition, the access latency based data offloading generates a fair schedule for the I_UAVs to offload data to the $Edge\_UAV$. Access latency ($R_i(t)$) of the i^{th} I_UAV_i in the time-slot t is the difference between the time of its last access by the $Edge\_UAV$ and the current time-slot.

$$\textbf{P2:} \quad \min_{X(t)} \sum_{t=1}^{T}\sum_{i=1}^{N} x_i(t) * ||S_{edge}(t+1) - S_{edge}(t)||^2$$

s.t.

$$||S_{edge}(t) - S_i(t)|| \le v_{max}\tau, \quad i = \{1..N\} \quad t\epsilon T (C1)$$
$$h_i^2(t) + ||S_{edge}(t) - S_i(t)||^2 \le g_o p_{max} (2^{\frac{d_i^{off}}{2W\tau}} - 1)^{-1} N_o^{-2} (C2)$$
$$Q_i(t) \ge 0, i\epsilon\{1..N\} (C3)$$
$$\sum_{i=0}^{N} (\frac{R_i(t)(1 - x_i(t)}{(N-1)}) \le R_{max}, i\epsilon\{1..N\} (C4)$$
$$\sum_{i=0}^{N} (x_i(t) * Q_i(t)) \ge 1, \quad i\epsilon\{1..N\} (C5)$$
$$\sum_{i=0}^{N} x_i(t) = 1 \quad i\epsilon 1..N (C6)$$

The first constraint $C1$ of optimization model $P2$ signifies the distance travelled within a time-slot is limited by the maximum velocity. The following constraint $C2$ restricts that the selected I_UAV_i should be in the coverage range of the $Edge\_UAV$. Constraint $C3$ denotes that the queue of the selected I_UAV_i shouldn't be empty while $C4$ limits the time that has elapsed since the last access of i^{th} I_UAV_i should be less than R_{max}. The constraint in $C5$ selects the I_UAV_i which has data to offload whereas $C6$

is a binary constraint to select only one of the I_UAV_i in a time-slot.

5 Lyapunov Optimization based System Stability

The model presented in **P1** in Section 3 is a stochastic optimization problem. The data arrival at the system queues is random in nature. With the help of online Lyapunov optimization algorithm, we can solve such stochastic optimization models and jointly stabilize all queues by finding the optimal $X(t)$ in each time slot [15].

The quadratic Lyapunov function [15] associates a scalar measure to queues of the system. Further, the stability of the system is maintained by a guaranteed mean rate stability of the evolving queues i.e.

$$\lim_{T\to\infty} \frac{\mathbb{E}[Q_i(t)]}{T} = 0, \forall i \in 1, 2, ..N \tag{8}$$

$$\lim_{T\to\infty} \frac{\mathbb{E}[L(t)]}{T} = 0 \tag{9}$$

$$Z(v(t)) = \frac{1}{2}\left[\sum_{i=1}^{N} Q_i(t)^2 + L(t)^2\right] \tag{10}$$

$v(t) = [\{Q_i(t)\}_{i=1}^{N}, L(t)]$ consists of all backlog queues of the system at time t and $Z(.)$ is quadratic Lyapunov function of system queues.

The **Lyapunov drift** corresponding to above function can be given as:

$$\triangle Z(v(t)) = E[(z(v(t+1)) - z(v(t)))] \tag{11}$$

The Lyapunov drift plus a penalty function is minimized to stabilize the queue backlog of the system which is given as:

$$\triangle D(t) = \triangle Z(v(t)) + V * \mathbb{E}[E_{system}(t)] \tag{12}$$

where V is a positive system constant which controls the trade-off between Lyapunov drift and the expected energy of the system. A high value of parameter V signifies more weight on minimizing energy of the system at the cost of high queue backlog. Hence, V acts as a trade-off parameter between system's energy and queue backlog.

An upper bound on $\triangle Z(v(t))$ can be derived as, (for details see [15, 11])

$$\begin{aligned} Z(v(t)) =& \mathbb{E}[-\sum_{i=1}^{N} Q_i(t) * d_i^{off}(t)] - \\ & \mathbb{E}[L(t) * (c(t) + d_{edge}^{off}(t))] + C \end{aligned} \tag{13}$$

where C is a deterministic constant.

As a result, the upper bound of the drift plus penalty function becomes

$$\begin{aligned} \triangle D(t) \leq C - \mathbb{E}[\sum_{i=1}^{N} Q_i(t) d_i^{off}(t) - L(t)(c(t) + r(t))] \\ + V * \mathbb{E}[E_{system}(t)|v(t)] \end{aligned} \tag{14}$$

Hence, the original formulation **P1** is reduced to **P3** which bounds the system's drift to keep the system stable as follows:

$$\begin{aligned} \mathbf{P3} \quad \min_{X(t)} & \mathbb{E}\left[-\sum_{i=1}^{N} Q_i(t) * d_i^{off}(t)\right] - \mathbb{E}[L(t)(c(t) \\ & + d_{edge}^{off}(t))] + V\mathbb{E}[E_{system}(t)] \end{aligned}$$

$$s.t.$$

$$0 \leq F_{ME}(t) \leq Fmax \quad t\epsilon T \quad (C1)$$

$$0 \leq p_i(t) \leq p_{i,max} \quad i = 1...N \quad t\epsilon T \quad (C2)$$

$$0 \leq P_{edge}(t) \leq P_{max} \quad t\epsilon T \quad (C3)$$

$$d_i^{off}(t) \leq Q_i(t) \quad i = 1..N \quad t\epsilon T \quad (C4)$$

$$c(t) \leq \frac{F_{max}\tau}{\rho_{edge}} \quad t\epsilon T \quad (C5)$$

$$d_i^{off} \leq W\tau log_2(1 + \frac{(\zeta)p_{i,max}(t)}{N_o * W}) i = 1..N \quad t\epsilon T \quad (C6)$$

$$d_{edge}^{off}(t) \leq W\tau log_2(1 + \frac{\zeta P_{max}(t)}{N_0 W}) \quad t\epsilon T \quad (C7)$$

As can be observed, the constraints in **P3** is a subset of the constraints in **P1**. To further simplify the solution of the optimization formulation, **P3** could be reformulated as two separate sub-problems provided the positions of $Edge\_UAV$ and I_UAV_i are fixed in a given time slot t.

5.0.1 Transmission energy optimization of I_UAVs

First sub-problem deals with the optimization of parameters related to the I_UAV_i. The variables $S_{edge}(t)$ i.e.

position of $Edge\_UAV$ and the offloaded bits of the selected I_UAV_i are coupled in particular time interval. The fixed position of $Edge\_UAV$ decouples these variables. In the optimization model **P 3.1**, the transmission energy is optimized for a single time-slot given the position of $Edge\_UAV$:

$$\textbf{P 3.1} \quad \min_{p_i(t)} -\sum_{i=1}^{N} Q_i(t) * d_i^{off}(t) + V * \sum_{i=1}^{N} p_i(t) * \tau$$

$$s.t.$$

$$0 \leq p_i(t) \leq p_{i,max} \quad i = 1..N \quad t \epsilon T$$

$$d_i^{off}(t) \leq Q_i(t) \quad i = 1..N \quad t \epsilon T$$

$$d_i^{off} \leq W * \tau log_2(1 + \frac{(\zeta) * p_{i,max}(t)}{N_o * W}) \quad i = 1...N \quad t \epsilon T$$

It can be observed that objective function in **P 3.1** is a convex function. First constraint is linear and the second constraint is upper bounded by a concave function. As a result, the stationary point of the objective function can be derived as: $p_i^*(t) = min\{max\{\frac{N_o}{\zeta}(\frac{Q_i(t)W}{V} + 1), 0\}, p_{max}\}$.

5.0.2 Transmission energy optimization of $Edge\_UAV$

The second sub-problem deals with the optimization of the $Edge\_UAV$ parameters for the amount of data offloaded to the cloud. Further, here we can ignore the processor frequency parameters and the associated constraints from the optimization as they do not affect the energy optimization. The updated optimization model is given as:

$$\textbf{P 3.2} \quad \min_{P_{edge}(t)} -L(t)(d_{edge}^{off}(t)) + VP_{edge}(t)\tau$$

$$s.t.$$

$$d_{edge}^{off} \leq L(t)$$

$$0 \leq P_{edge}(t) \leq P_{max}$$

$$r(t) \leq W\tau log_2(1 + \frac{\zeta P_{max}(t)}{N_o W}) \quad t \epsilon T$$

The model **P 3.2** has a convex optimization objective subject to convex constraints to solve the optimal transmission power of the $Edge\_UAV$. The stationary point of the optimization model **P 3.2** is $P_{edge}(t) = \frac{N_0}{\zeta}(\frac{L(t)W\tau}{V} - 1)$.

The overall solution approach of the proposed heterogeneous multi-UAV framework is given in Algorithm 1.

Algorithm 1 Heterogeneous Multi-UAV Framework

Input: Trajectories of all I_UAV_i and list of PoIs l_i.
Time, $t = 0$

while $t \leq T$ **do**
1. Estimate the $\{Q_i(t)\}_{i=1}^{N}$and $\{S_i(t)\}_{i=1}^{N}$
2. Select the i^{th} I_UAV_i to offload data using P2
3. Compute and offload $d_i^{off}(t)$ for I_UAV_i using P 3.1 to $Edge\_UAV$
4. Update $Q_i(t)$
5. Transmit status message to $Edge\_UAV$
6. Compute and offload $d_{edge}^{off}(t)$ as using P 3.2
7. Update $L(t)$
8. t=t+1

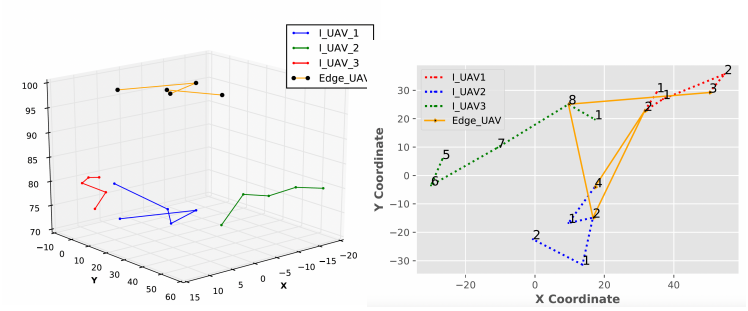

(a) (b)

Figure 1: (a) **3D Trajectory of UAVs** (b) **Top View of Trajectory of I_UAVs and $Edge\_UAV$ for 10 timeslots with Latency markers**

6 Experimentation

In this section, we present the simulation setup to validate the efficacy of our proposed Distance and Latency Aware Trajectory Optimization with Lyapunov based system utility. The pre-computed trajectories of each of the I_UAV_i are shared with the $Edge\_UAV$ before the simulation starts. The simulation parameters are listed in Table 1.

We have considered a 100m x 100m square region with PoIs at 2m distance and at heights ranging from 70m to 80m. There are total 2500 PoIs in the region. We sample 500 PoIs uniformly at random. Simulation were performed using three I_UAV_i and one $Edge\_UAV$. All

Table 1: **Simulation parameters**

Parameters	Values
Channel Bandwidth	1000MHz
Image size	1 Mb or above
Maximum Transmit Power	120 Watts
Effective switched capacitance	10^{-28}
Noise Power N_0	10^{-12}
Cycles required	30 cycles per bit
The path-loss constant g_0	10^{-4}
Path loss exponent θ	2 to 4
Maximum access latency	4-10
Queue limit of I_UAV	1000MB

the I_UAV_i start from randomly selected PoIs of a geographic cluster. The sequence of PoIs visited by each I_UAV_i is generated using the following steps: 1) Assign all the I_UAV_i to randomly selected PoIs of a geographic cluster. 2) All the I_UAV_i select the nearest non-visited PoIs one after the other. This continues till all PoIs are visited. 3) Before proceeding to the next PoI, an I_UAV_i collects all the data ($A_i(t)$) from that PoI. In this process of data collection, an I_UAV_i may remain at the same PoI across multiple time-slots until all the data ($A_i(t)$) is collected. For each PoI, the visual data to be collected is modelled as the number of bits randomly sampled from a Gaussian distribution with mean as 800 Kb and variance as 200 Kb. We conducted separate experiments for low data and high data scenarios. For low data, the amount of data at each PoI is two times the output of Gaussian distribution while for high data, the amount of data to be collected is 8 times of the Gaussian distribution.

The optimization parameter V ranges from 10 to 10^{15}. The length of each time slot is 60 seconds. Figure 1a shows a section of the 3D view of the trajectories followed by the I_UAV_i and $Edge\_UAV$. Figure 1b shows the top view of the same with the access latency depicted at each location point. For better illustration, we have selected a sequence of 10 time slots to draw the trajectory. As can be observed in Figure 1b, for I_UAV_3 the access latency increases from 5 at location (-26,5.7) to 8 (upper threshold) at location (9,25). Afterwards, the I_UAV_3 gets accessed by the $Edge\_UAV$ resulting in the decrease of access latency to 1 at location (17,19) in the next time slot.

In order to validate the performance of our proposed framework, we created a baseline approach for both the

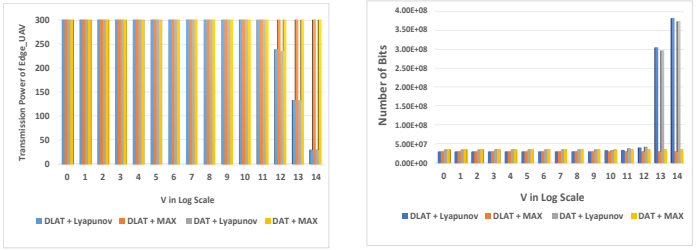

(a) Average Edge UAV Transmission Power consumption (b) Average Edge UAV Queue length

Figure 2: Experimental Results on Transmission power and Queue Length

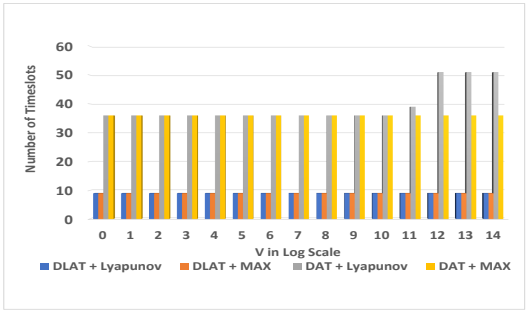

Figure 3: Comparison of maximum Access Latency

broad categories of the optimization problems viz.: 1) Trajectory Optimization and 2) Transmission Energy and system stability.

7 Results and Discussions

In this section, we discuss the comparative performances of our proposed approach with other baselines.

7.1 Influence of the trade-off parameter V on $Edge\_UAV$

Figure 2a depicts effect of the increase in the parameter V with respect to the transmission power of the $Edge\_UAV$. It is evident that DLAT + MAX and DAT + MAX always consume the maximum energy which makes the average energy consumption same across different values of V. For

DAT + Lyapunov and DLAT + Lyapunov, a drop in the energy consumption can be observed for V values of 11, 12 and 13. In the Figure 2b, it can be seen that the average $Edge\_UAV$ queue length stays low for both DLAT + MAX and DAT + MAX at all the values of V. For DAT + Lyapunov and DLAT + Lyapunov, we can observe that the average queue length of $Edge\_UAV$ starts to increase around V = 11, 12 and 13. It is to be noted that the deflection points in the Figure 2a and Figure 2b align with each other.

In the Figure 2b, the average queue length of $Edge\_UAV$ increases with increase in V as the weightage of the system utility increases. The DLAT and DAT methods with Lyapunov shows similar performance whereas the MAX approach is not affected with the change in the trajectory optimization.

7.2 Per Time slot analysis of I_UAV_i

As shown in Figure 4 [a], per time slot data offloading schedule of I_UAV_i based on the trajectory of $Edge\_UAV$ incurs higher access latency for DAT based approaches. Besides this, Figure 4 [b] shows that the queue of I_UAV_i is higher for the DAT combinations throughout. It is interesting to note from these results that the queue utilization in DLAT combinations is well spread out keeping the energy consumption less for optimal V. However, for DAT combinations the queue utilization is more bursty in nature and so is the energy consumption which even touches the MAX baseline for some time-slots as shown in Figure 4 [c]. This behavior can be explained by the fact that in the DAT based approaches, the $Edge\_UAV$ selects the nearest I_UAV which may not have sufficient data to offload at that time instant. On the other hand, the DLAT based approaches select the I_UAVs optimally considering the distance as well as the data availability in the I_UAV queues.

Hence, it can seen that our proposed DLAT + Lyapunov shows consistently better performances with optimally balanced trade-off between the trajectory optimization with low access latencies and minimal transmission power consumption of the system.

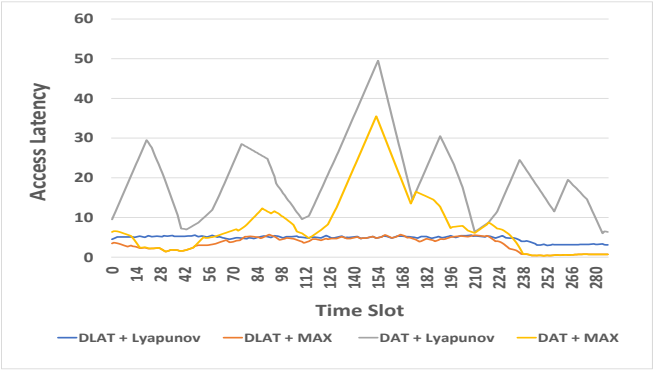

(a) Maximum Access Latency

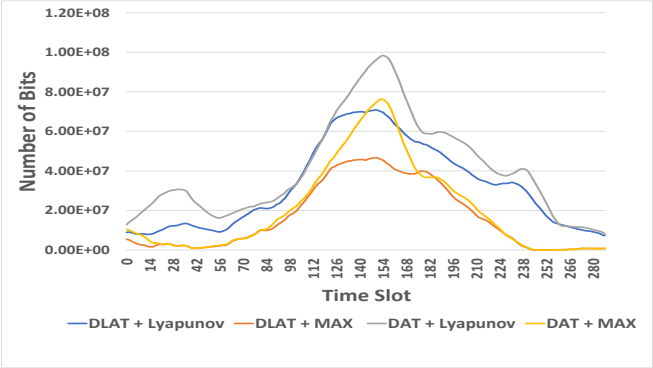

(b) Maximum Buffer

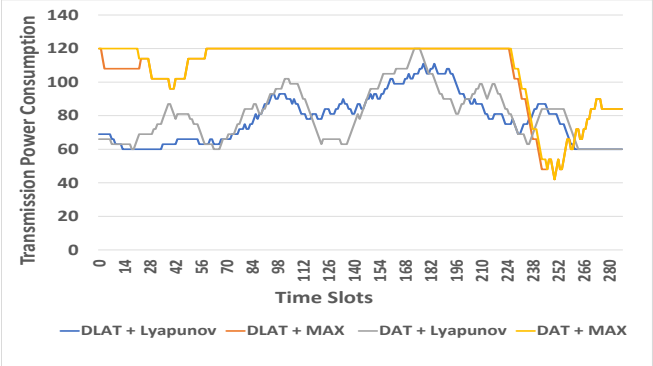

(c) Maximum Power Transmission

Figure 4: **Analysis of I_UAV per time slot**

8 Conclusion

UAV based applications for progress monitoring and resource tracking are emerging in construction industry.

Constructions projects have minimal infrastructure for capture and offloading of ground-truth data. This paper presents a heterogeneous multi-UAV based framework for end-to-end data collection and offloading using a distance and latency aware trajectory optimization. The Lyapunov optimization approach is used to ensure the stability of the system in terms of expected system queue backlogs by breaking the system optimization problem into two subproblems. The simulation results show that the access latency of our proposed (DLAT + Lyapunov) approach performs better than other baseline approaches. Moreover, the analysis of system parameter V has shown a trade-off between the queue stability and the system utility.

References

[1] M. Mozaffari, W. Saad, M. Bennis, Y.-H. Nam, and M. Debbah, "A tutorial on uavs for wireless networks: Applications, challenges, and open problems," *IEEE communications surveys & tutorials*, vol. 21, no. 3, pp. 2334–2360, 2019.

[2] F. Ruggiero, V. Lippiello, and A. Ollero, "Aerial manipulation: A literature review," *IEEE Robotics and Automation Letters*, vol. 3, no. 3, pp. 1957–1964, 2018.

[3] A. D. Boursianis, M. S. Papadopoulou, P. Diamantoulakis, A. Liopa-Tsakalidi, P. Barouchas, G. Salahas, G. Karagiannidis, S. Wan, and S. K. Goudos, "Internet of things (iot) and agricultural unmanned aerial vehicles (uavs) in smart farming: A comprehensive review," *Internet of Things*, p. 100187, 2020.

[4] S. Waharte and N. Trigoni, "Supporting search and rescue operations with uavs," in *2010 International Conference on Emerging Security Technologies*. IEEE, 2010, pp. 142–147.

[5] H. Hamledari, S. Davari, S. O. Sajedi, P. Zangeneh, B. McCabe, and M. Fischer, "Uav mission planning using swarm intelligence and 4d bims in support of vision-based construction progress monitoring and as-built modeling," in *Construction Research Congress 2018*, 2018, pp. 43–53.

[6] Y. Mao, C. You, J. Zhang, K. Huang, and K. B. Letaief, "A survey on mobile edge computing: The communication perspective," *IEEE Communications Surveys & Tutorials*, vol. 19, no. 4, pp. 2322–2358, 2017.

[7] M. Golparvar-Fard, F. Peña-Mora, and S. Savarese, "Integrated sequential as-built and as-planned representation with d 4 ar tools in support of decision-making tasks in the aec/fm industry," *Journal of Construction Engineering and Management*, vol. 137, no. 12, pp. 1099–1116, 2011.

[8] V. Nguyen, T. T. Khanh, P. Van Nam, N. T. Thu, C. S. Hong, and E.-N. Huh, "Towards flying mobile edge computing," in *2020 International Conference on Information Networking (ICOIN)*. IEEE, 2020, pp. 723–725.

[9] S. Wan, J. Lu, P. Fan, and K. B. Letaief, "Towards big data processing in iot: Path planning and resource management of uav base stations in mobile-edge computing system," *IEEE Internet of Things Journal*, 2019.

[10] N. Abbas, Y. Zhang, A. Taherkordi, and T. Skeie, "Mobile edge computing: A survey," *IEEE Internet of Things Journal*, vol. 5, no. 1, pp. 450–465, 2017.

[11] M. Neely, *Stochastic network optimization with application to communication and queueing systems*. Morgan & Claypool Publishers, 2010.

[12] J. Zhang, L. Zhou, Q. Tang, E. C.-H. Ngai, X. Hu, H. Zhao, and J. Wei, "Stochastic computation offloading and trajectory scheduling for uav-assisted mobile edge computing," *IEEE Internet of Things Journal*, vol. 6, no. 2, pp. 3688–3699, 2018.

[13] A. Al-Hourani, S. Kandeepan, and S. Lardner, "Optimal lap altitude for maximum coverage," *IEEE Wireless Communications Letters*, vol. 3, no. 6, pp. 569–572, 2014.

[14] J. Lu, S. Wan, X. Chen, Z. Chen, P. Fan, and K. B. Letaief, "Beyond empirical models: Pattern formation driven placement of uav base stations," *IEEE Transactions on Wireless Communications*, vol. 17, no. 6, pp. 3641–3655, 2018.

[15] M. J. Neely, *Network Optimization: Notes and Exercises*, 2018. [On-

line]. Available: http://ee.usc.edu/stochastic-nets/docs/network-optimization-notes.pdf